^{2}H, ^{3,4}He($\vec{p}$,p') and ^{3,4}He($\vec{p}$,d') continuum yields for 100 and 150 MeV protons

J. S. Wesick,* P. G. Roos, N. S. Chant, C. C. Chang, A. Nadasen,† L. Rees,‡ and N. R. Yoder§
Department of Physics and Astronomy, University of Maryland, College Park, Maryland 20742

A. A. Cowley and S. J. Mills
Council for Scientific and Industrial Research, National Accelerator Centre, Faure, South Africa

W. W. Jacobs
Indiana University Cyclotron Facility, Bloomington, Indiana 47405
(Received 22 April 1985; revised manuscript received 8 July 1985)

The continuum cross sections and analyzing powers from the ^{2}H, ^{3,4}He($\vec{p}$,p') and ^{3,4}He($\vec{p}$,d') reactions were measured for 98.7 and 149.3 MeV polarized protons in the angular range 17.5° to 60°. The ^{2}H and ^{3}He data show strong quasifree contributions with more ambiguous results for ^{4}He. These data are compared with distorted-wave impulse approximation calculations based on quasifree nucleon and deuteron knockout. Overall, the agreement between theory and experiment is moderately good. However, some significant discrepancies are observed and corrections to the simple model are discussed.

I. INTRODUCTION

For many years it has been observed that proton continuum spectra arising from intermediate energy proton-nucleus reactions often show a broad peak described as the quasifree scattering peak. This peak is generally assumed to arise from nucleon-nucleon (N-N) scattering, its location and width being determined by a combination of nucleon-nucleon kinematics, the Fermi motion of the target nucleons, and the separation energy of the various shells in the target nucleus. The quasifree peak becomes more pronounced with increasing bombarding energy: There is no evidence for a quasifree peak at 62 MeV (Ref. 1); at 90 and 100 MeV (Ref. 2) a quasifree peak is observed only at the most forward angles; at much higher bombarding energy the quasifree peak dominates the (p,p') spectra and at 800 MeV,[3] in conjunction with the quasifree peak arising from pion production[4] ($N + N \rightarrow N + N + \pi$), represents essentially all of the reaction cross section, in agreement with the impulse approximation treatment of nucleon-nucleus scattering. Further support of the quasifree interpretation is obtained from the facts that at 90 MeV the ratio of the (p,p') to (p,n') cross sections[5] is very close to that predicted for N-N scattering; and (p,2p) correlation studies at 100 MeV (Ref. 6) and 200 MeV (Ref. 7) on ^{58}Ni indicate that quasifree N-N scattering is the dominant first stage in any proton-nucleus interaction.

Inclusive studies carried out with other projectiles also show strong quasifree peaks. For example, both (e,e') reactions[8] and (π,π') reactions[9] exhibit very pronounced quasifree peaks for a range of target nuclei. The quasifree peaks for these projectiles tend to be more pronounced than those of (p,p') reactions, except at the highest proton energies. In the case of (e,e'), this presumably represents the fact that multiple scattering is unimportant for the electrons. For (π,π') the pronounced quasifree peak may be due to the strong absorption of the pion restricting the pion yield to only surface nucleons.

The experimental study of these quasifree peaks has two possible useful aspects—nuclear structure and reaction dynamics. Complete knowledge of the reaction dynamics would allow one to extract information on the momentum components of the nucleons in the nucleus. Although this has been attempted, the complexity of the reaction dynamics for all reactions greatly limits its usefulness. From a reaction dynamics standpoint it is clear that any reaction channel which accounts for a majority of the reaction cross section should be understood and included in the framework of theoretical models. At a more sophisticated level is the understanding of the quasifree scattering itself, and the modifications required to theory for effects such as those due to the nuclear medium.

The theoretical description of quasifree scattering has evolved from early plane wave impulse approximation calculations for (p,p') at 320 MeV (Ref. 10) by Wolff[11] based on a (p,pN) mechanism. Later Kroll and Wall[12] included distortion effects in an approximate manner using a WKB approximation. More exact calculations of (e,e') assuming (e,ep) collisions have been carried out[13] and show the importance of describing the unobserved continuum proton in a proper potential. The most recent attempts[14] to fit (π,π') data also include propagation of an intermediate Δ.

In the present experiment we have measured the cross sections and analyzing powers at a limited number of angles for the continuum arising from the interaction of 100 and 150 MeV protons with ^{2}H and ^{3,4}He. It was our hope to help clarify the importance of quasifree scattering in the energy range near 100 MeV, where there appears to be a transition from multiple scattering dominance to dominance by quasifree N-N scattering. The few nucleon targets were chosen: (a) to minimize contributions from multiple scattering, (b) to remove essentially all of the evaporation contribution, (c) to minimize contributions

from high-lying collective states, and (d) to examine the changes in the spectra resulting from changes in the number of target nucleons, and hence small but rapidly changing multiple scattering. Furthermore, the analyzing power data, which has seldom been measured, provides additional constraints on the theoretical models. In particular, it was hoped that near zero analyzing powers in the spectrum could be used as a signature of multiple scattering dominance. In fact, this was not the case. However, the analyzing power data is most useful, and is the clearest signature of the presence of deuteron knockout. In Sec. II we describe the experimental procedure and in Sec. III present the experimental results.

We have then compared these experimental data with distorted-wave impulse approximation (DWIA) calculations assuming (p,pn) and (p,2p) reactions. The calculations include significant improvements over previous (p,p') calculations based on nucleon knockout. The theoretical model is presented in Sec. IV, and compared to the experimental data in Sec. V.

II. EXPERIMENTAL DESCRIPTION

Polarized proton beams of 98.7 and 149.3 MeV were obtained from the Indiana University cyclotron with an average current of approximately 20 nA and an average beam polarization of 75%. These beams were delivered to a 163 cm diameter scattering chamber containing the targets and detector systems. The target consisted of a 12.7 cm diameter gas cell with 7.6 μm Havar entrance and exit windows. The cell was filled with $>99\%$ purity ^{2}H, ^{3}He, and ^{4}He gases to approximately 1 atm pressure and the temperature and pressure of the cell were monitored continuously during the course of the experiment. The emergent charged particles were detected by two counter telescopes each consisting of a 1 mm Si surface barrier ΔE detector followed by a 5.1 cm diameter, 7.6 cm thick NaI crystal E detector.

The slit systems in front of each of these detectors consisted of a double collimator system to eliminate particles originating in the gas cell windows for angles greater than approximately 12°. Each collimator consisted of a Ta slit and a plastic scintillator active collimator with a hole, the solid angle and target length being defined by the active collimators. The angular resolution of each telescope was approximately 1.6° and the gas target length for 90° was approximately 8.9 mm.

For each telescope fast signals were obtained using a charge sensitive preamplifier with a fast pickoff for the ΔE detectors and by differentiating the dynode pulse from the NaI crystal photomultiplier. A coincidence

$$(\Delta E \cdot E \cdot \overline{\text{Front Collimator} \cdot \text{Rear Collimator}})$$

with approximately 50 ns resolving time was formed for each telescope and used to define a valid event. The linear ΔE and E signals were matched, added, and the sum $(E+\Delta E)$ and the ΔE signal sent through linear gates gated by the coincidence requirement. The output was sent to a Tennelac PACE system interfaced to a Harris on-line computer.

Computer softwave windows were set around each particle type and the energy spectra for protons, deuterons, and tritons stored in 1024 channel computer analyzers. In addition, the ΔE vs $E+\Delta E$ spectrum was stored in a 64×64 channel array. At the end of each run data were transferred to magnetic tape.

For each angle the two telescopes were placed at equal angles on opposite sides of the beam, and the spin of the beam flipped every 2 min. For this geometry the analyzing power was calculated using the expression

$$A=\frac{1}{\bar{P}}\frac{\sqrt{x}-1}{\sqrt{x}+1}\,, \tag{1}$$

where $x=L_+R_-/R_+L_-$ and $\bar{P}=\frac{1}{2}(P_++P_-)$. Here P_+ and P_- are the polarizations of the incident beam for spin up $(+)$ and spin down $(-)$, and L and R refer to the left and right detectors. By using two detectors and two spin orientations possible systematic errors cancel in first order. The error in analyzing power for expression (1) is given by

$$\Delta A=\frac{1}{\bar{P}}\left[\frac{x}{(1+\sqrt{x})^4}\left(\frac{1}{L_+}+\frac{1}{L_-}+\frac{1}{R_+}+\frac{1}{R_-}\right)+A^2(\Delta P)^2\right]^{1/2}, \tag{2}$$

where ΔP is the error in measuring $\bar{P}$.

During the course of the experiment pulser signals triggered by the Faraday cup integrator were sent to each preamplifier and used to measure dead time. The beam polarization was monitored every few runs and varied by at most a few percent. Data were taken at several angles for $\vec{p}+p$ scattering and used as tests of the normalization as well as for energy calibration purposes. In addition, elastic proton scattering from ^{2}H, ^{3}He, and ^{4}He was compared to previous measurements when possible. The absolute cross sections agreed to within 10% with previous measurements. At 100 MeV the analyzing powers agree with recent $p+{}^4$He measurements.[15] At 150 MeV the analyzing powers were on the average about 15% smaller in magnitude than those in the previous measurements.[16] Since some of the previous analyzing power data may be less reliable, we present our analyzing power data as measured.

One difficulty which arises for the small angle data is the contribution to the continuum from the elastic scattering reaction tail in the NaI crystal. This reaction tail has a modest effect on the cross section data, but can have significant impact on the continuum analyzing power data. The reaction tail was subtracted by hand using the results for $p+{}^4$He. In this case the 20 MeV breakup threshold allows one to extract the reaction tail contribution near the elastic scattering peak. We also measured the contribution at lower proton energies where the ΔE signal is sufficient to separate the reaction tail from the true continuum. Assuming the reaction tail contribution varies linearly between these two points and with ^{4}He as a template, the subtraction was carried out for ^{2}H and ^{3}He. This subtraction was necessary only for the 17.5° and 30° points and the error introduced was included in the data.

Reaction tail contributions from other parts of the spectra are negligible.

The uncertainty in normalization of the absolute cross section scale is approximately 10%. The errors presented in the figures are relative errors only.

III. EXPERIMENTAL DATA

Data were obtained at 100 MeV at 17.5°, 30°, 45°, and 60° for all three targets. At 150 MeV data were obtained at two or three of these angles. The continuum cross sections and analyzing powers are presented in Figs. 1—6 along with theoretical calculations which will be discussed in Sec. IV. Note that for these figures (and subsequent figures where applicable) theoretical calculations were performed only at selected values of the energy, and lines to guide the eye are drawn through the symbols representing theoretical cross sections and analyzing powers. Experimental cross section data are indicated by solid lines with error bars where appropriate.

The ^{2}H and ^{3}He data all show a strong quasifree peak whose centroid nicely follows nucleon-nucleon kinematics. At small angles the large low energy tail is suggestive of a multiple scattering. In the case of ^{4}He, there is no pronounced quasifree peak which shifts with nucleon-nucleon kinematics. Just above the breakup threshold one sees

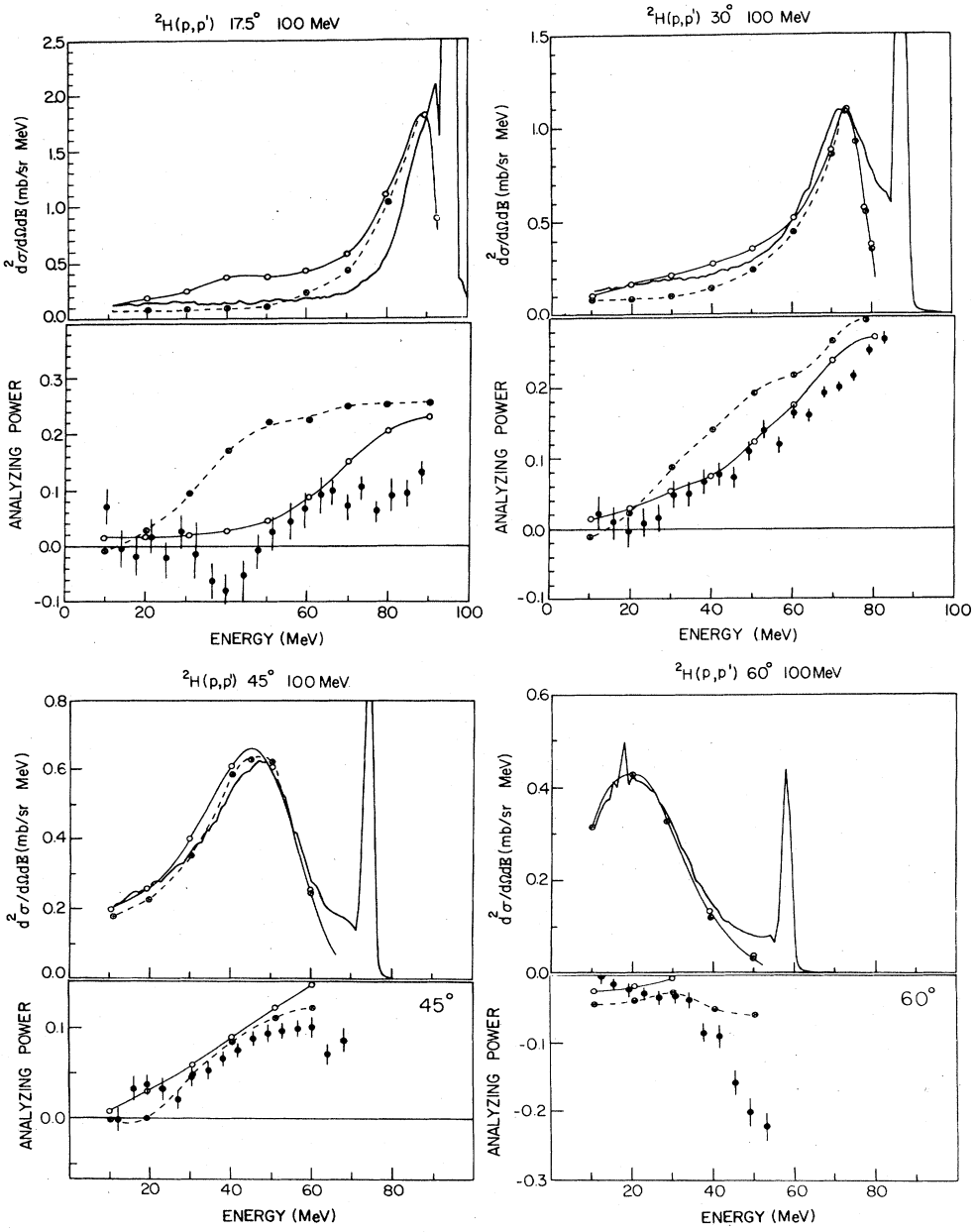

FIG. 1. ^{2}H(p,p') inclusive cross sections and analyzing powers at 98.7 MeV. The curves are PWIA calculations with different on-shell prescriptions for the nucleon-nucleon cross sections (—○—, FEP; ——●——, IEP) (see Sec. V).

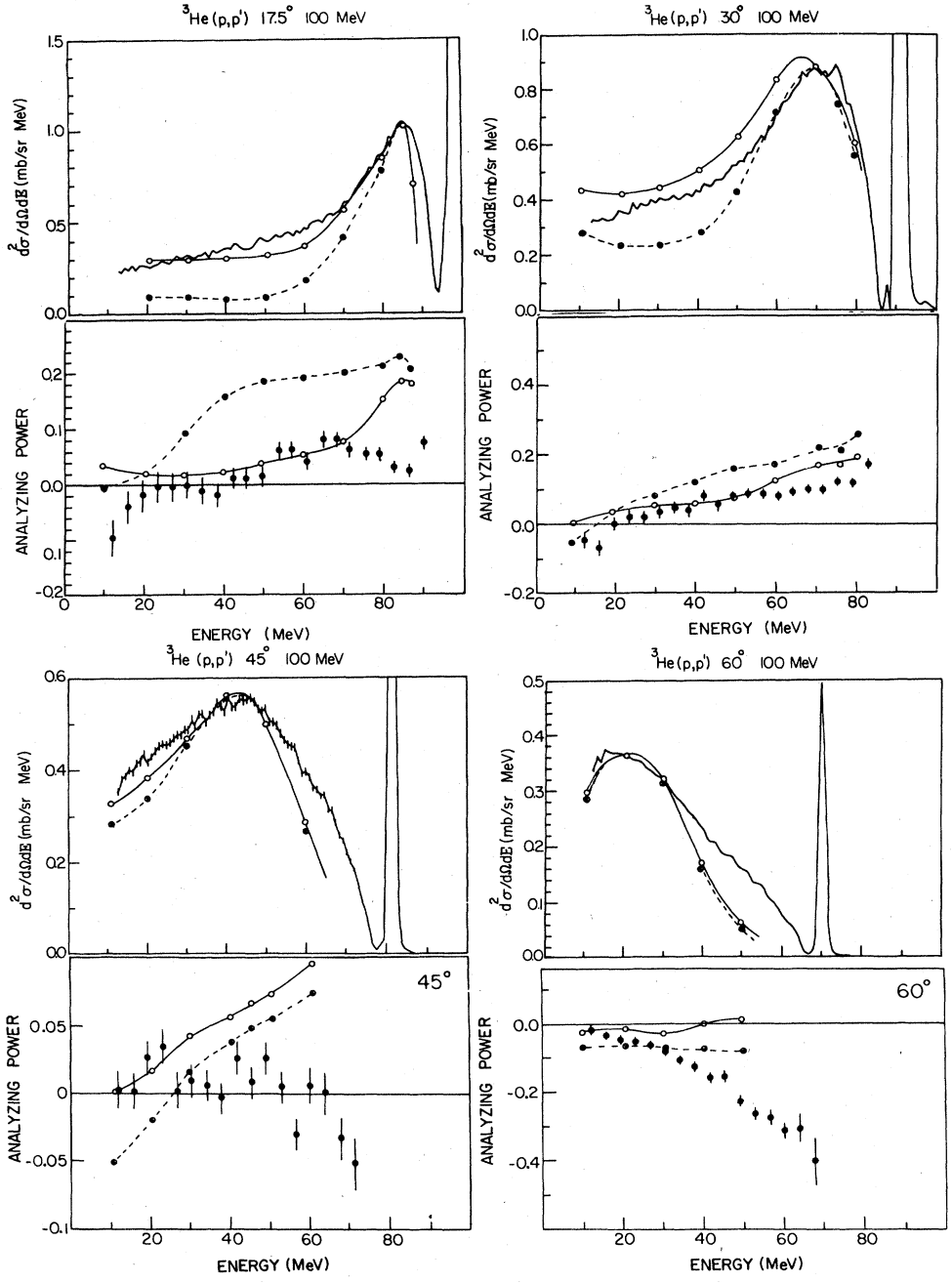

FIG. 2. ^{3}He(p,p') inclusive cross sections and analyzing powers at 98.7 MeV. The curves are DWIA calculations (—○—, FEP; ——●——, IEP) (see Sec. V).

clear evidence of inelastic scattering to unbound states in ^{4}He, and it is possible that several states contribute to distort the upper end of the continuum spectrum. The continuum cross section falls as the target mass increases from ^{2}H to ^{4}He, presumably reflecting the increase in the width of the single-particle momentum space wave function due to increased nucleon separation energy.

The analyzing power data show similar trends for all target nuclei, apart from the 17.5° ^{2}H data at 100 MeV which seems to be somewhat overcompensated for the reaction tail contribution around 50 MeV. In general, the analyzing power is approximately zero for low outgoing proton energy, its magnitude gradually increasing with the outgoing proton energy. As a function of angle the analyzing powers are positive at forward angles, go through zero near 45°, and become negative at 60°. This is a result one might predict assuming N-N scattering from a stationary target nucleon. Furthermore, at 17.5° and 30°

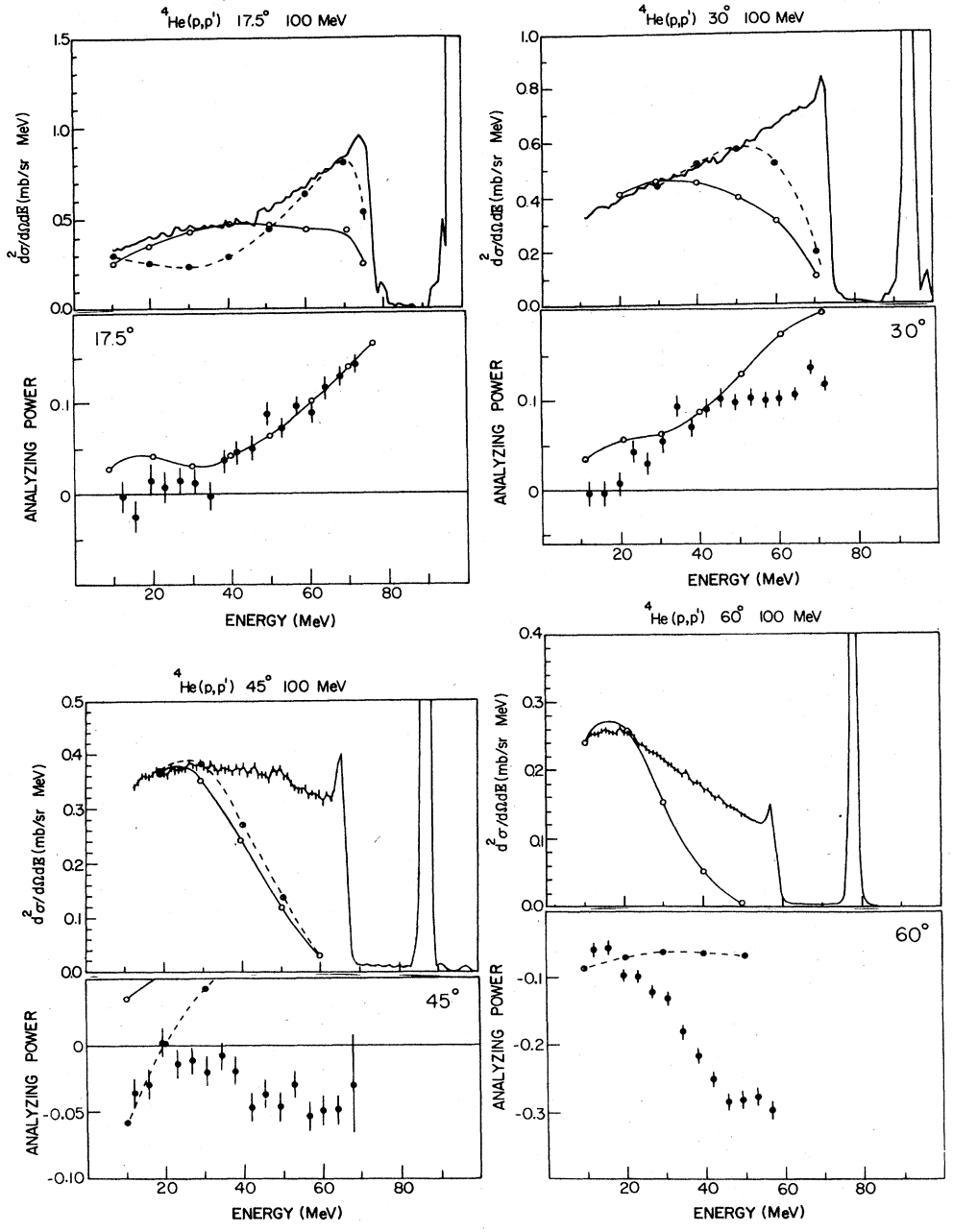

FIG. 3. ^{4}He(p,p') inclusive cross sections and analyzing powers at 98.7 MeV. The curves are DWIA calculations (—○—, FEP; ——●——, IEP) (see Sec. V).

the analyzing powers for ^{2}H are larger than those for ^{3}He. Again, based on nucleon-nucleon scattering since the $\vec{p}+n$ $A(\theta)$ is larger than the $\vec{p}+p$, this effect is not unexpected. The ^{4}He analyzing powers are close to those of ^{2}H at 17.5° and close to those of ^{3}He at 30°. Finally, $A(\theta)$ increases with bombarding energy as expected for N-N scattering.

To show the angular and mass dependence of the analyzing power more clearly we present $A(\theta)$ extracted from the data at the predicted location of the quasifree peak. This result is shown in Fig. 7 along with the N-N analyzing power for each bombarding energy. It is clear that the general trend is that of N-N scattering.

IV. THEORETICAL MODEL

A number of theoretical models have been utilized in the analysis of (p,p') inclusive data. These models range from preequilibrium exciton models[17] to cascade models[18] based on nucleon-nucleon scattering to PWIA and DWIA

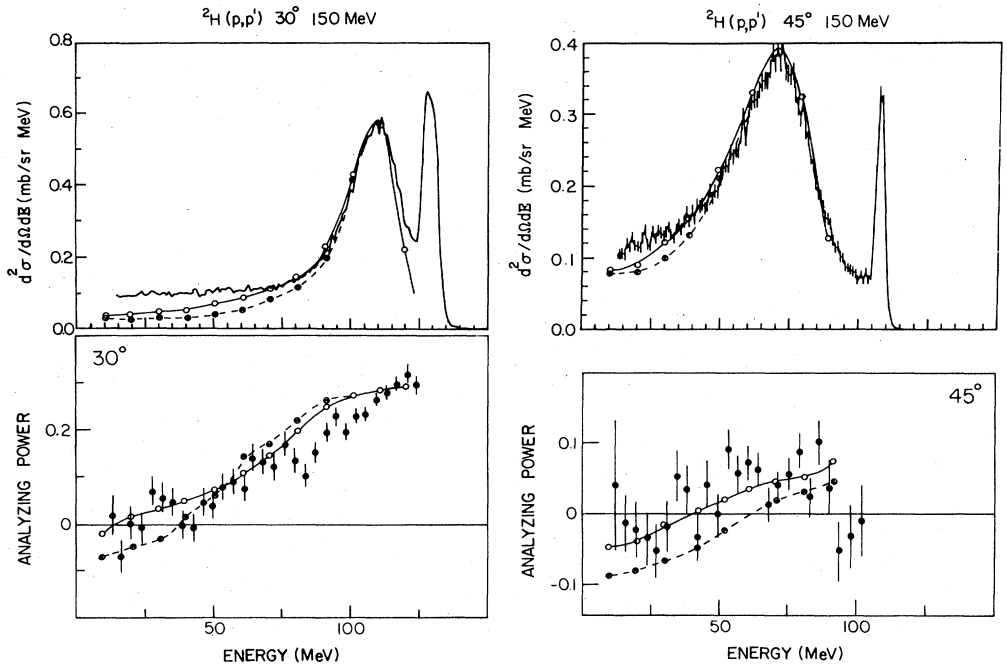

FIG. 4. ^{2}H(p,p') inclusive cross sections and analyzing powers at 149.3 MeV. The curves are PWIA calculations (—○—, FEP; ——●——, IEP) (see Sec. V).

calculations[3,11,12] of (p,pN). For the present energies and few nucleon targets we would expect the last two approaches to be the most reasonable. The cascade model and the DWIA are similar in concept but with some fundamental differences. For example, the cascade model is a semiclassical model and assumes straight line trajectories between nucleon-nucleon collisions. In addition, the representation of the target nucleus wave function is generally poor, often being taken from a Fermi gas model. On the other hand, the cascade model can make quantitative predictions of the multiple scattering effects allowing more than two free particles in the final state.

DWIA calculations include the wave nature of the incoming and outgoing nucleons and allow one to utilize a variety of single-particle wave functions. However, such calculations do not allow one to make quantitative predictions for multiple scattering leading to three-nucleon final states. In the DWIA multiple scattering is included only for three-body final states where the incoming or outgoing nucleons can elastically scatter from the residual core.

We have chosen to analyze the present data with the DWIA, a theoretical treatment which has been rather successful in predicting exclusive (p,2p) and (p,pn) transitions to discrete states.[19] We have carried out calculations using a factorized DWIA without the additional approximations made in Refs. 11 and 12. Our hope was to carry out the best possible calculation for three-body final states, and then by comparison with the data test the accuracy of the model and attempt to identify the effects of multiple scattering.

In the factorized DWIA,[20] neglecting spin-orbit terms in the distorted waves, the A(p,pN)B cross section for the knockout of a nucleon with quantum numbers (n,l,j) into solid angles $d\Omega_p, d\Omega_N$ with energy E_p can be written in the schematic form

$$\frac{d^3\sigma}{d\Omega_p d\Omega_N dE_p} = \mathrm{KF} \times C^2S \times \frac{d\sigma}{d\Omega}\bigg|_{p\text{-}N} \times \left|\sum_\lambda T^{\alpha l\lambda}\right|^2 , \tag{3}$$

where KF is a known kinematic factor and C^2S is the spectroscopic factor for the final state in the residual nucleus and represents the probability of finding a nucleon to eject. The two-body cross section $d\sigma/d\Omega\,|_{p\text{-}N}$ is properly a half-off-the-mass shell cross section which is generally approximated by an on-shell cross section. The quantity $T^{\alpha l\lambda}$ is the distorted momentum distribution

$$T^{\alpha l\lambda} = \frac{1}{(2l+1)^{1/2}} \int \chi_p^{(-)*}(\mathbf{r})\chi_N^{(-)*}(\mathbf{r})\phi_{nlj}(\mathbf{r}) \times \chi_0^{(+)}\left[\frac{B}{A}\mathbf{r}\right] d^3r , \tag{4}$$

where the χ's are the incoming and outgoing nucleon distorted waves and ϕ_{nlj} the bound nucleon single-particle wave function in the nucleus. In the plane wave limit $T^{\alpha l\lambda}$ is simply the Fourier transform of the single-particle wave function.

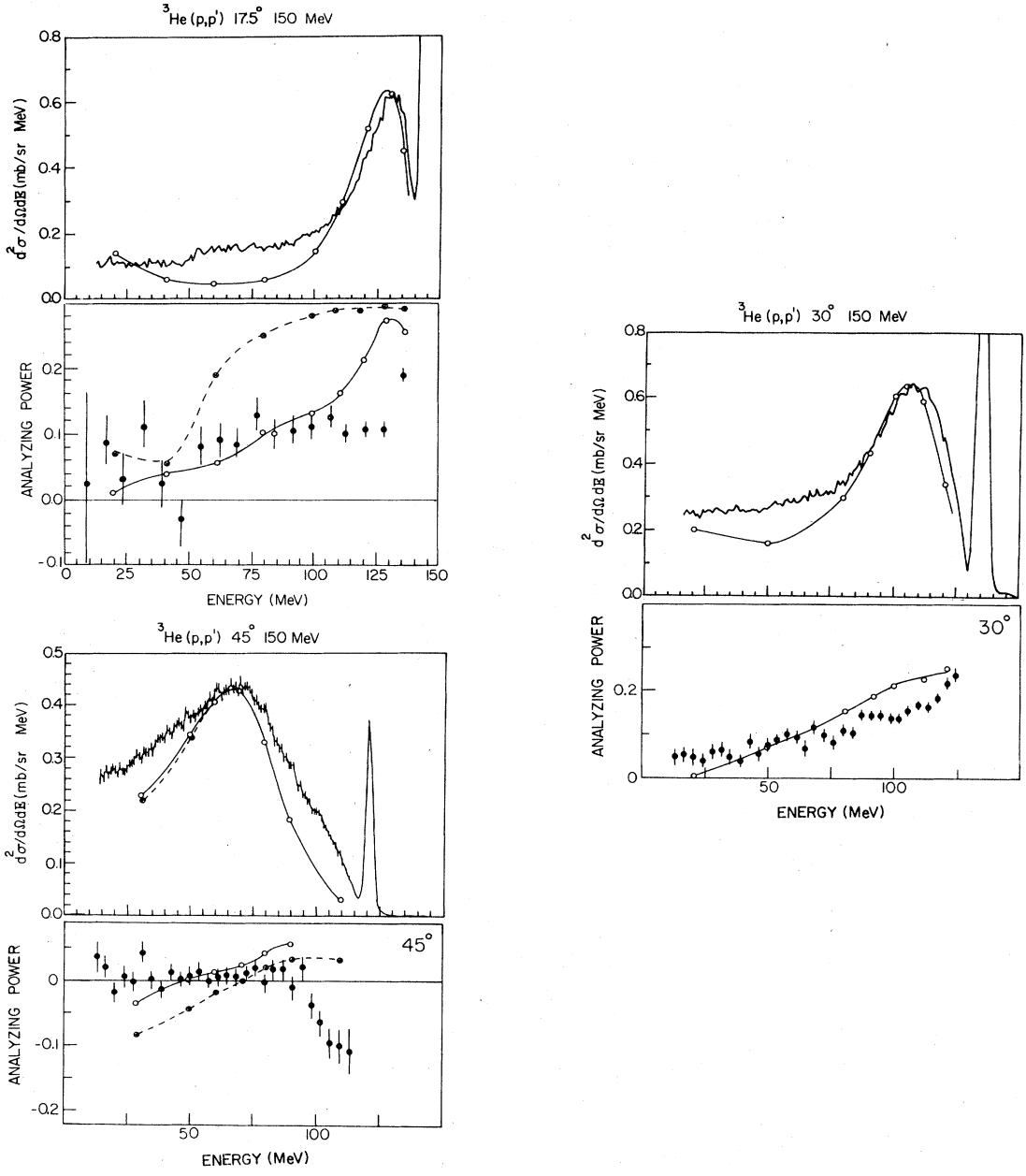

FIG. 5. ^{3}He(p,p') inclusive cross sections and analyzing powers at 149.3 MeV. The curves are DWIA calculations (—o—, FEP; ——●——, IEP) (see Sec. V).

Equation (3) describes a (p,pN) process in which the region of phase space occupied by the ejected nucleon is defined. To describe inclusive data based on this (p,pN) model it is necessary to integrate over $d\Omega_N$, the solid angle of the unobserved nucleon. Thus, the double differential cross section becomes

$$\frac{d^2\sigma}{d\Omega_p dE_p} = \int \frac{d^3\sigma}{d\Omega_p dE_p d\Omega_N'} d\Omega_N' \,. \tag{5}$$

Furthermore, since one of the particles is unobserved, the optical potential used to describe the wave cannot be complex. This wave should be calculated in a purely real potential.[13] Note that in this model, as opposed to other models of the continuum such as the slab model,[21] the Pauli blocking is naturally included, since the kinematics and phase space factors require the unobserved nucleon to make a transition into the continuum.

Since for the present targets only S-state nucleon knockout is allowed and we are ignoring spin-orbit distortions, the analyzing power for (p,pN) is simply the p-N

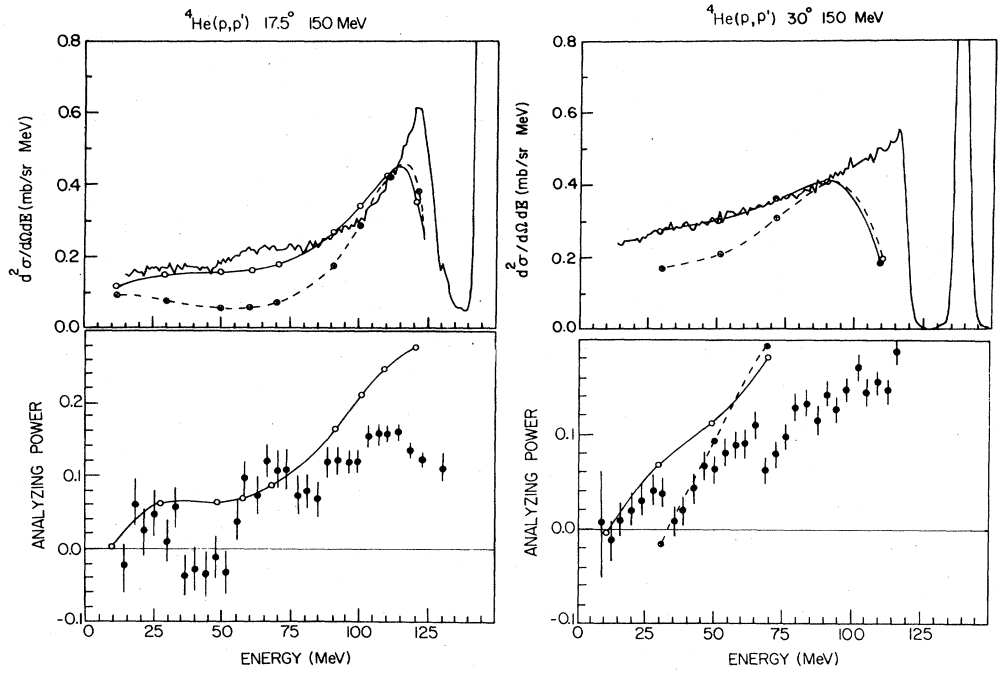

FIG. 6. ^{4}He(p,p') inclusive cross sections and analyzing powers at 149.3 MeV. The curves are DWIA calculations (—○—, FEP; ——●——, IEP) (see Sec. V).

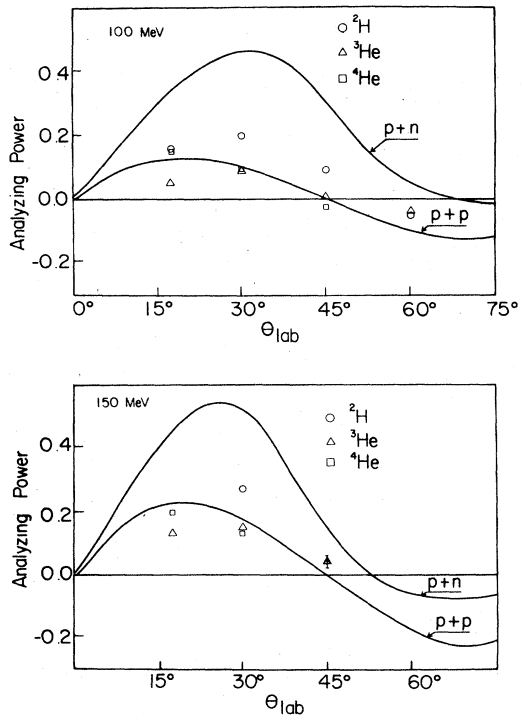

FIG. 7. Analyzing powers at the quasifree peak from the data in Figs. 1—6. The curves represent free p + p and p + n analyzing powers.

analyzing power.[22] Thus, the ($\vec{p}$,p') continuum analyzing power for the proton with energy E_p entering solid angle $d\Omega_p$ is given by

$$A(\Omega_p,E_p)=\frac{\int A(\text{p-N})\dfrac{d^3\sigma}{d\Omega_p d\Omega_N dE_p}d\Omega_N}{\int \dfrac{d^3\sigma}{d\Omega_p d\Omega_N dE_p}d\Omega_N}, \qquad (6)$$

where A(p-N) is the two-body p + N analyzing power appropriate for the (p,pN) reaction. Previous calculations of ($\vec{p}$,2p) have shown spin-orbit distortions to generally

TABLE I. Wave functions of bound nucleon.

d

$$\phi(r)=\frac{1}{\beta-\alpha}\left[\frac{\alpha\beta(\alpha+\beta)}{2\pi}\right]^{1/2}\frac{e^{-\alpha r}-e^{-\beta r}}{r}$$

$\alpha=0.232$ fm^{-1}, $\beta=1.434$ fm^{-1}

^{3}He

$\phi(r)=C(\alpha/2\pi)^{1/2}(1-e^{-\beta' r})^4 e^{-\alpha r}/r$

$C=1.73$, $\alpha=0.4201$ fm^{-1}, $\beta'=1.90$ fm^{-1}

^{4}He

$\phi(r)=C(\alpha/2\pi)^{1/2}(1-e^{-\beta' r})^4 e^{-\alpha r}/r$

^{4}He-n $C=4.35$, $\alpha=0.9631$ fm^{-1}, $\beta'=1.20$ fm^{-1}

^{4}He-p $C=4.26$, $\alpha=0.8463$ fm^{-1}, $\beta'=1.20$ fm^{-1}

have a rather small effect,[22,23] but we will examine these later for several cases.

Calculations were carried out for both $(\vec{p},2p)$ and $(\vec{p},pn)$ using the code THREEDEE of Chant. The integral over $d\Omega_N$ was carried out by the use of Gauss-Legendre quadrature with 12 to 20 points for each integration. Plane wave calculations were used to determine the range of $d\Omega_N$ over which to integrate and that a suitable number of Gaussian points were included for the DWIA calculations. The resultant cross sections were then added, incoherently weighted by the number of target nucleons of each type. Numerical uncertainties in the DWIA calculations are believed to be less than 10%.

For ^{2}H a Hulthen bound nucleon wave function, and for both ^{3}He and ^{4}He Eckart form bound-state wave functions were used with parameters taken from the work of Lim.[24] The parameters for these wave functions are given in Table I. The optical-model parameters used in the calculation were taken from optical-model fits to elastic scattering data[25,26] with the imaginary potential taken to be zero for the unobserved particle.

For the two-body half-shell cross sections $d\sigma/d\Omega\,|_{p\text{-}N}$ we have used two standard on-shell prescriptions: the final energy prescription uses the N-N cross section corresponding to the final relative energy of the two outgoing nucleons; the initial energy prescription corresponds to the relative energy of the two-nucleon system before the collision. For these two prescriptions the two-body cross section was calculated by interpolating experimentally determined N-N phase shifts. For the $(\vec{p},2p)$ calculations we used n-n cross sections rather than p-p cross sections. The use of the p-p cross sections occasionally caused large unphysical spikes in the calculations. These arise due to the Coulomb potential whenever $d\sigma/d\Omega\,|_{p\text{-}p}$ needed to be evaluated at angles near 0° or 180°. We argue that use of the n-n cross section is more in the spirit of the impulse approximation. The Coulomb interaction is long range and is thus more properly treated as a distortion of the incoming projectile rather than an impulsive interaction which can eject a nucleon.

V. COMPARISON OF THEORY AND EXPERIMENT

A. Effects of on-shell prescription and distortion

The calculations have a variety of components which we first investigate separately. In Fig. 2 we present DWIA cross sections and analyzing powers for ^{3}He$(\vec{p},p')$ with both the initial energy (IEP) and final energy (FEP) prescriptions for the two-body N-N t matrix. At 100 MeV the choice of prescriptions makes fairly modest changes in both magnitude and shape of the cross section; the magnitude changing by 15% to 30%. At 30° there is little difference in $A(\theta)$ while at 60° the IEP is somewhat more negative than the FEP and hence more closely resembles the data. This is not surprising since the elastic p-n analyzing powers become negative at smaller angles as the incident energy is increased.

In Fig. 8 we present the theoretical results for ^{3}He at 100 MeV for the FEP, but with the contributions of $(\vec{p},2p)$ and $(\vec{p},pn)$ separated. For a single nucleon we see that neutron knockout produces a somewhat larger cross section. More importantly, the $A(\theta)$ differ significantly; the neutron knockout being much larger at 30°, and remaining positive at 60°. This larger (p,pn) $A(\theta)$ is, however, diluted by the proton contributions in the case of ^{3}He. Note that at low energies the sampling of the two-body t matrix created by the integral over the unobserved

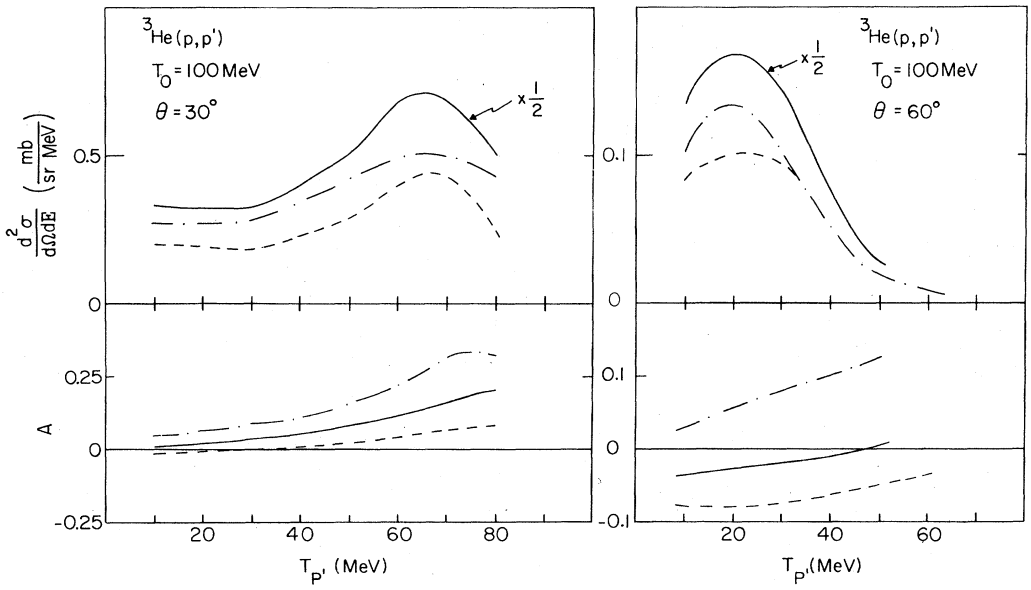

FIG. 8. DWIA calculations for ^{3}He(p,p') at 100 MeV. The solid curve corresponds to the final energy prescription. The additional two curves show the individual contributions from one proton (———) or one neutron (—·—·) knockout.

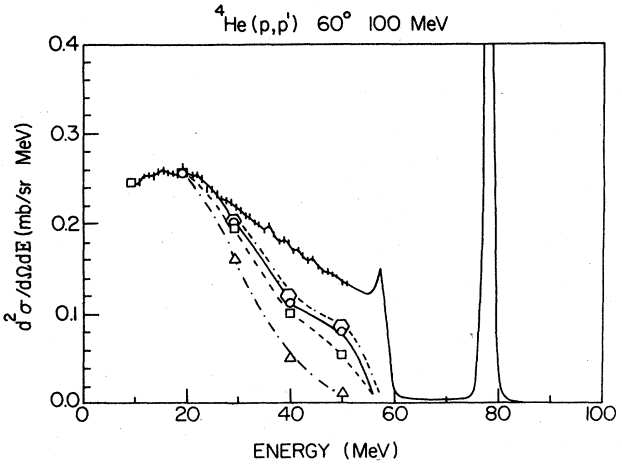

FIG. 9. Calculations for ^{4}He(p,p') at 98.7 MeV using the initial energy prescription. The curves correspond to different treatments of the distortion with the indicated normalization factors (———□, PWIA×0.73; —○, DWIA with the undetected nucleon in a purely real potential ×1.86; —·—△, DWIA with an undetected nucleon plane wave ×2.24; ——·——●, DWIA with the undetected nucleon in a complex potential ×2.85).

nucleon significantly reduces the analyzing power. Thus, even the single scattering mechanism gives rise to a very small $A(\theta)$ and the small $A(\theta)$ for low energy protons cannot be used as a signature of multiple scattering.

Finally, we look at the distortion effects. In Fig. 9 we present calculations of ^{4}He(p,p') at 100 MeV, the case with largest distortion effects. Only calculations for the IEP are shown. Clearly distortion effects are important but not dominant for these few nucleon targets. Introduction of distorted waves (with no absorption for the undetected particle) reduces the cross section by about a factor of 2.5 and tends to broaden the spectrum. The analyzing powers, however, are relatively unaffected by the distortion effects. This is not unexpected. If the distortion effects are relatively constant over the range of integration of $d\Omega_N$ the distortion effects factor as a ratio DWIA/PWIA. Thus, the analyzing power does not change.

For $\theta_{lab}=60°$ we have also included calculations in which the undetected particle was described using (i) a plane wave, (ii) the wave function for a particle scattered from a pure real potential, or (iii) a wave function for a particle scattered from a complex potential. The third case would correspond to an experiment in which both the final state nucleons were detected. One observes that the use of plane waves does change the spectrum. Furthermore, the use of a complex potential reduces the theoretical cross section by about 30%.

In the case of ^{2}H(p,p') we will present only PWIA calculations in comparison to experiment, since a few sample calculations showed distortions to have little effect on the shape and primarily affect the maximum by reducing it by roughly 30%.

B. Comparison of conventional DWIA calculations to experiment

In Figs. 1—6 the DWIA calculations (PWIA for ^{2}H) are compared to the experimental results. In each case the theoretical cross section has been normalized to the experimental data at the quasifree peak. The normalization constants are shown in Fig. 10.

For ^{2}H(p,p') the fits to the cross sections and $A(\theta)$ are generally quite good. There appears to be some preference for the FEP at the forward angles, changing to the IEP at the larger angles. At the largest angle (60°) the $A(\theta)$ becomes quite negative at the highest detected energies. The elastic scattering $A(\theta)$ is negative, but the contribution from the reaction tail is negligible. Rather, this negative $A(\theta)$ probably reflects final state interactions between unobserved n-p systems, due to the $^1S_0$ n-p resonance.

The normalization factors are near unity but tend to increase with angle. Considering the simplicity of the bound wave function these differences from unity are probably not unreasonable. The variation with angle will

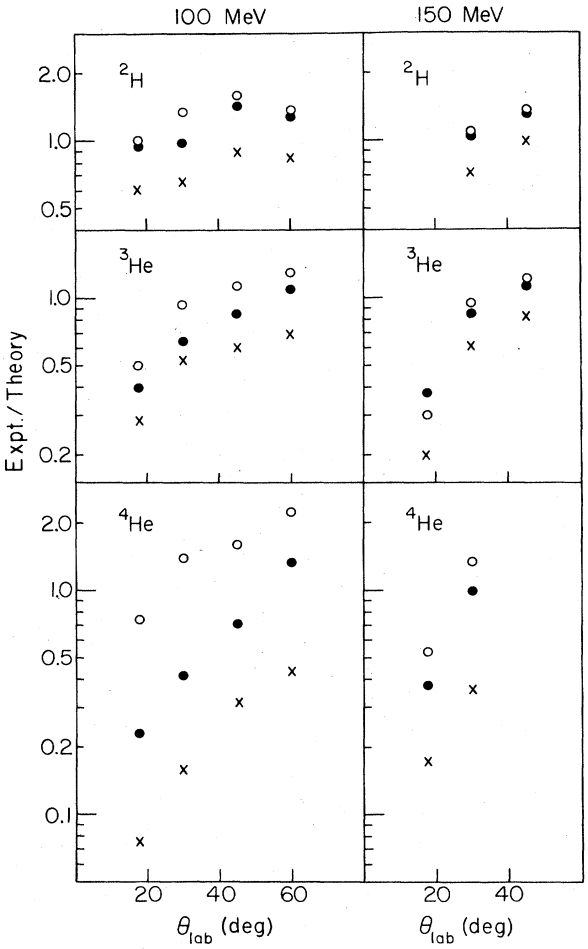

FIG. 10. Ratio of experimental to theoretical cross section as normalized in Figs. 1—6 (×, PWIA with FEP; ●, DWIA with FEP; ○, DWIA with IEP).

be addressed further after discussing the results for all three targets.

For ^{3}He(p,p′) the overall fits to the cross section and $A(\theta)$ are also rather good, and the behavior is similar to ^{2}H. At the larger angles the calculated energy distribution is narrower than the data. This may be due to a poor representation of the single-particle wave function in momentum space, although this wave function does fit elastic electron scattering to high momentum transfer. The low energy side probably arises from multiple scattering, but the excess on the high energy side is somewhat surprising.

As in the ^{2}H(p,p′) case we find that the $A(\theta)$ becomes quite negative at 60° for high energy outgoing protons. This is not predicted by our present DWIA calculations.

The normalization factors for ^{3}He(p,p′) are also presented in Fig. 10. The behavior of the normalization is similar to that of ^{2}H; viz., the theoretical cross sections fall more rapidly than the experimental data. However, in this case the variation is more rapid, changing by about a factor of 2.5 over the angular range of the experiment.

Finally, for ^{4}He(p,p′) we have the difficulty that we never observe a clean quasifree peak. The theoretical calculations have been normalized to the data at the expected location of the quasifree peak. The calculations produce a broad quasifree peak, but the data always have additional large contributions at the high energy end of the spectra. A likely source of these contributions is inelastic scattering to highly excited states in ^{4}He. Another source of high energy protons is from the knockout of heavier particles which is addressed in Sec. V C.

The $A(\theta)$ are similar to those for d and ^{3}He and are described fairly well with again the exception of 60° where the $A(\theta)$ is large and negative. The normalizations, at least in the sense that calculations are normalized at the location of the quasifree peak, show the same angular dependence as the other two targets.

C. Corrections to DWIA

Some serious deficiencies exist in our theoretical description of the experimental data. We have examined several possibilities in an attempt to improve the theoretical description. The elastic scattering $A(\theta)$ arising from the optical-model spin-orbit potential are large and become negative at 60°. Although previous calculations[22,23] suggest that spin-orbit effects are small, we carried out several calculations including spin-orbit potentials in the optical-model potentials for the incoming and outgoing nucleons. In general the effects on the cross section are very small, producing of the order of a 10% change. For ^{3}He at 60° the effect of the spin-orbit potential actually worsens the agreement with the analyzing power data. Thus, spin-orbit effects are ineffective in explaining the discrepancies in normalization to the cross section or $A(\theta)$.

A second possibility is that contributions due to the knockout of clusters of nucleons, such as (p,pd), may be important. PWIA calculations, as described in Sec. III, for (p,pd) reactions were carried out for ^{3}He and ^{4}He. The needed p + d two-body cross sections and $A(\theta)$ were obtained by interpolation of a variety of experimental measurements.[27] Due to the lack of adequate high quality experimental data, this interpolation is crude but sufficient to test the importance of such contributions. The bound deuteron wave function for ^{3}He was taken to be the same as the bound proton wave function with a spectroscopic factor $C^2S=\frac{3}{2}$. For ^{4}He→d + d a harmonic oscillator wave function deduced from the ^{4}He(p,pd) work of Frascaria *et al.*[28] was used. Since this is not a microscopic description, we have had to add the resultant (p,pd) calculation *incoherently* to the previous PWIA nucleon knockout results, and normalize to the experimental data.

At forward angles the contribution from (p,pd) is small and produced little change in the previously presented results, except that it tends to fill in the high energy portion of the cross section. However, at large angles the fact that the $\vec{p}$ + d $A(\theta)$ is large and negative, combined with the fact that the (p,pd) quasifree peak lies at a higher outgoing proton energy, has a large effect. In Fig. 11 we show the calulations for ^{3}He and ^{4}He at 60°. Calculations with either the initial energy or final energy prescriptions for the two-body cross section give comparable results. The inclusion of deuteron knockout improves agreement with the high energy portion of the cross section. In this respect we note that inclusion of the (p,pt) reaction should contribute to even higher energies, and thus perhaps the unusually flat spectra associated with ^{4}He arise due to contributions from cluster knockout. More importantly, the (p,pd) contribution leads to a large negative $A(\theta)$ in the high energy portion of the spectrum where it dominates over (p,pN).

It is clear that inclusion of (p,pd) tends to correct at least two of the major discrepancies noted before. It leads to the large negative $A(\theta)$ at 60° and tends to fill in the high energy portion of the cross section spectra. However, when included at all angles it does not remove the angular dependence of the normalization factor.

Although the improved agreement shown in Fig. 11 is suggestive that the source of the original discrepancies observed is the (p,pd) contribution, we can make a further test by direct comparison with the ($\vec{p}$,d′) spectra. These spectra should come primarily from detecting the deuteron from ($\vec{p}$,pd). Typical results for ^{3,4}He($\vec{p}$,d′) are shown in Figs. 12 and 13. For ^{3}He we have also added incoherently a contribution for the ^{3}He(p,d)2p final state using a Watson-Migdal description of the final state interaction. The calculations show good qualitative agreement with the experimental data. The occasional rapid change in the theoretical curves arise from interpolating the sparse $\vec{p}$ + d data.

The normalizations of the cross section data are shown in Fig. 14. We note that although there is again an angular dependence, the normalizations are about the same (within a factor of 2) as those for the (p,p′) spectra. Thus we conclude that a major component of the yield in the high energy portion of the ^{3,4}He(p,p′) spectra arises from the (p,pd) reaction, and that it is most likely this reaction which leads to the large negative $A(\theta)$.

The problem with the angular dependent normalization, however, remains. Although reminiscent of Pauli block-

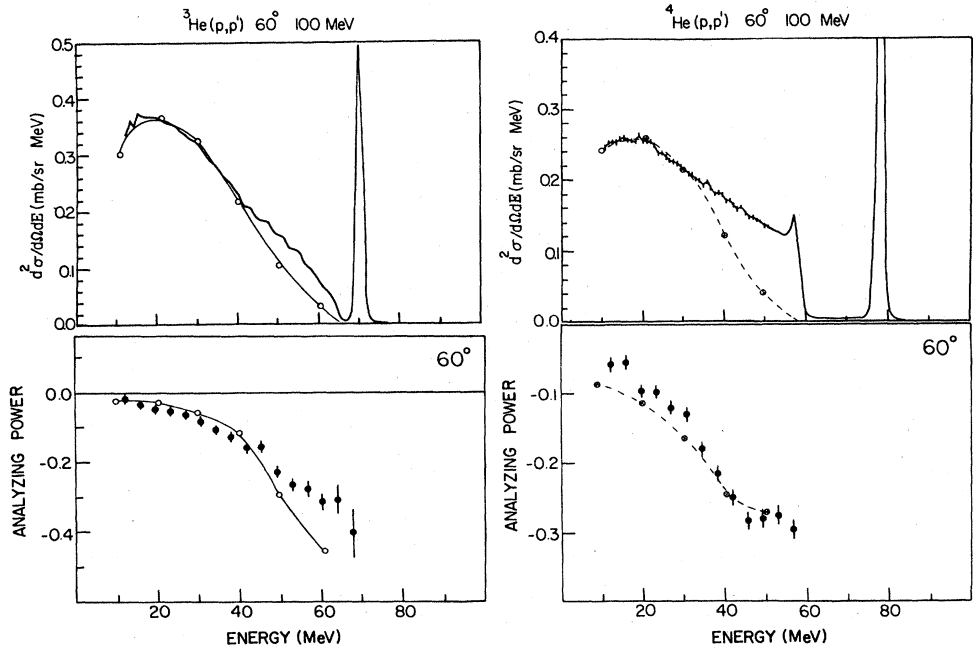

FIG. 11. ^{3,4}He(p,p') cross sections and analyzing powers at 98.7 MeV. The curves are PWIA calculations for both (p,pN) and (p,pd) added incoherently (—○—, FEP; —●—, IEP).

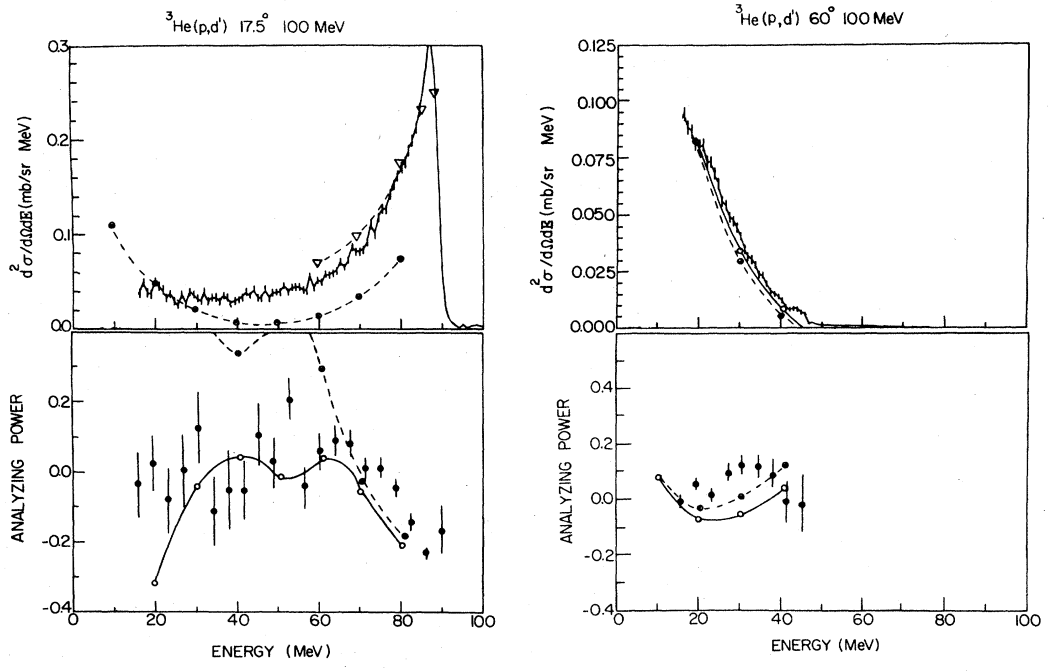

FIG. 12. Typical ^{3}He(p,d') spectra. The curves are PWIA calculations (—○—, FEP; —●—, IEP; —▽—, IEP plus Watson-Migdal).

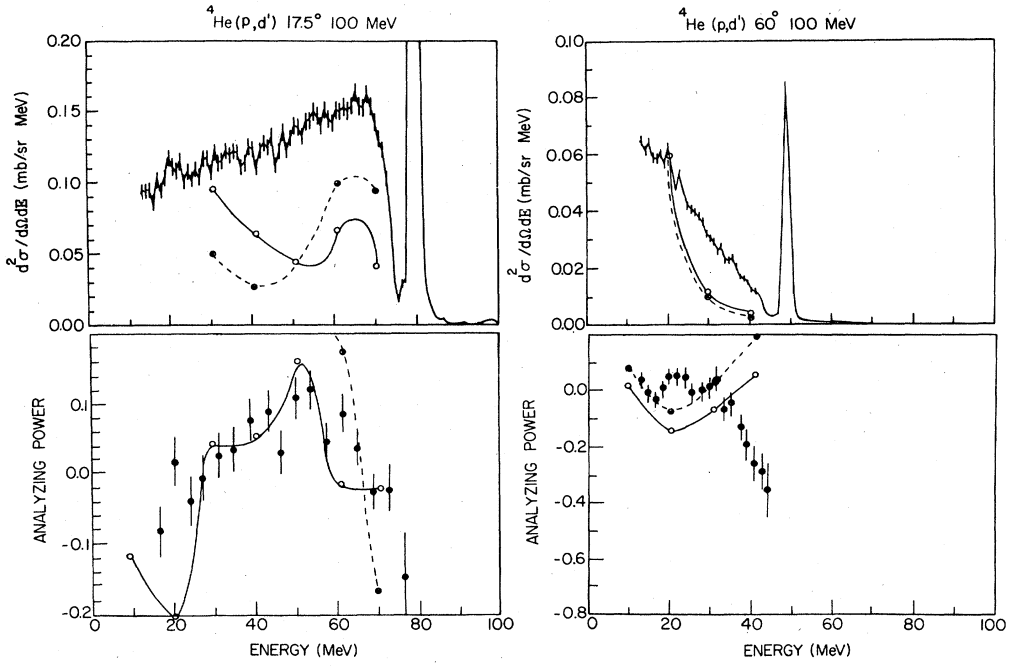

FIG. 13. Typical ^{4}He(p,d') spectra. The curves are PWIA calculations (—○—, FEP; ——●——, IEP).

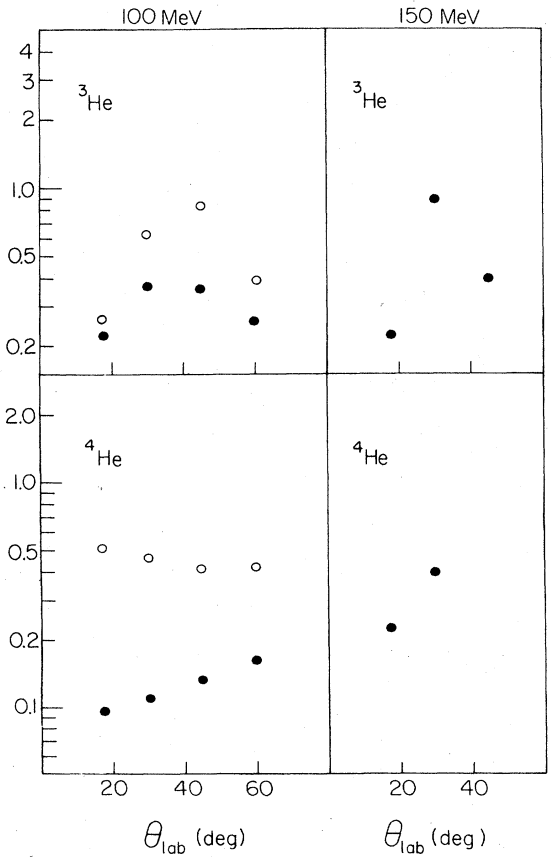

FIG. 14. Ratio of experimental to theoretical cross sections for ^{3,4}He(p,d'). (●, PWIA with FEP; ○, PWIA with IEP.)

ing effects, these are included in the present theoretical model, at least at the kinematic level.

VI. SUMMARY AND CONCLUSIONS

Measured cross sections and analyzing powers for the ^{2}H, ^{3,4}He($\vec{p}$,p') and ^{3,4}He(p,d') continuum have been compared to DWIA calculations. Overall the agreement between theory and experiment is moderately good, suggesting the dominant importance of single step nucleon-nucleon collisions. However, discrepancies between experiment and theory based on single nucleon knockout clearly indicate the need for including deuteron knockout for the light target nuclei, as well as possibly triton knockout.

In spite of improved agreement with inclusion of cluster knockout, a major problem still exists in that the normalization is angular dependent. Several sources of this discrepancy are possible. Firstly, it is perhaps questionable to apply distorted-wave techniques to such light systems where the relatively few number of open channels may give rise to relatively strong interference effects. Presently ^{12}C($\vec{p}$,p') and ^{58}Ni($\vec{p}$,p') data, which involve many more open reaction channels, are being analyzed with the same model to examine whether similar discrepancies exist.

Secondly, an improvement to the code to include half-off-shell cross sections in the calculation is presently being made. Calculations of the N-N half-shell cross section suggest that this inclusion may lead to some improvement. However, until they are included in the integral over the unobserved particle which causes the N-N t matrix to be sampled over a relatively large range of variables, the overall effect is not known.

Finally, the fact that DWIA calculations are approxi-

mately a factor of 2 smaller than PWIA indicates multiple scattering effects are not large but are significant. For these light targets these multiple scattered nucleons can appear in our measured spectra (i.e., they do not become thermalized and appear in an evaporation peak). Thus, it may be that the multiple scattered particles appear in the low energy part of the spectrum and lead to an enhanced yield at larger angles. This effect would suggest that the normalization at forward angles is most correct. The fact that this normalization is less then unity is probably not particularly significant considering the simplicity of the single nucleon wave functions. With respect to this we note that normalization of ^{3}He(p,2p) calculations to 100 MeV experimental data gives rise to a normalization of 0.65, which is comparable to the forward angle normalizations in ^{3}He(p,p'). The question of multiple scattering affects can be most easily addressed by carrying out coincidence measurements.

Overall the agreement between theory and experiment is encouraging. However, the extraction of significant quantitative information from such quasielastic studies must await more sophisticated theoretical analyses.

ACKNOWLEDGMENTS

We wish to thank the University of Maryland Computer Science Center for its generous support. This work was supported in part by the National Science Foundation.

*Present address: TRIUMF, Vancouver, British Columbia, Canada V6T 2A3.

†Present address: Department of Natural Sciences, University of Michigan—Dearborn, Dearborn, MI 48128.

‡Present address: Los Alamos National Laboratory, Physics Division, MS-D434, Los Alamos, NM 87545.

§Present address: Indiana University Cyclotron Facility, Bloomington, IN 47405.

[1]F. E. Bertrand and R. W. Peelle, Phys. Rev. C **8**, 1045 (1973).

[2]J. R. Wu, C. C. Chang, and H. D. Holmgren, Phys. Rev. C **19**, 698 (1979).

[3]R. E. Chrien, T. J. Krieger, R. J. Sutter, M. May, H. Palevsky, R. L. Stearns, T. Kozlowski, and T. Bauer, Phys. Rev. C **21**, 1014 (1980).

[4]J. A. McGill, G. W. Hoffmann, M. L. Barlett, R. W. Fergerson, E. C. Milner, R. E. Chrien, R. J. Sutter, T. Kozlowski, and R. L. Stearns, Phys. Rev. C **29**, 204 (1984).

[5]B. D. Anderson, A. R. Baldwin, A. M. Kalenda, R. Madey, J. W. Watson, C. C. Chang, H. D. Holmgren, R. W. Koontz, and J. R. Wu, Phys. Rev. Lett. **46**, 226 (1981).

[6]A. A. Cowley, C. C. Chang, H. D. Holmgren, J. D. Silk, D. L. Hendrie, R. W. Koontz, P. G. Roos, C. Samanta, and J. R. Wu, Phys. Rev. Lett. **45**, 1930 (1980).

[7]G. Ciangaru, C. C. Chang, H. D. Holmgren, A. Nadasen, P. G. Roos, A. A. Cowley, S. Mills, P. P. Singh, M. K. Saber, and J. R. Hall, Phys. Rev. C **27**, 1360 (1983); G. Ciangaru, C. C. Chang, H. D. Holmgren, A. Nadasen, and P. G. Roos, *ibid.* **29**, 1289 (1984).

[8]For example, R. R. Whitney, I. Sick, F. R. Ficenec, R. D. Kephart, and W. P. Trower, Phys. Rev. C **9**, 2230 (1974); J. S. McCarthy, I. Sick, R. R. Whitney, and M. R. Yearian, *ibid.* **13**, 712 (1976).

[9]For example, C. H. Q. Ingram, P. A. M. Gram, J. Jansen, R. E. Mischke, J. Zicky, J. Bolger, E. T. Boschitz, G. Pröbstle, and J. Arvieux, Phys. Rev. C **27**, 1578 (1983).

[10]J. B. Cladis, W. N. Hess, and B. J. Moyer, Phys. Rev. **87**, 425 (1952).

[11]P. A. Wolff, Phys. Rev. **87**, 434 (1952).

[12]F. R. Kroll and N. S. Wall, Phys. Rev. C **1**, 138 (1970).

[13]Y. Horikawa, F. Lenz, and Nimai C. Mukhopadhyay, Phys. Rev. C **22**, 1680 (1980).

[14]Michael Thies, Nucl. Phys. **A382**, 434 (1982).

[15]A. Nadasen, private communication.

[16]H. Postma and R. Wilson, Phys. Rev. **121**, 1229 (1961); K. Kuroda, A. Michalowicz, and M. Poulet, Phys. Lett. **13**, 67 (1964); K. Kuroda, A. Michalowicz, M. Poulet, and F. Gomez-Gimeno, *ibid.* **16**, 133 (1965); N. P. Goldstein, A. Held, and D. G. Stairs, Can. J. Phys. **48**, 2629 (1970); H. Langevin-Joliot, Ph. Narboni, J. P. Didelez, G. Duhamel, L. Marcus, and M. Roy-Stephan, Nucl. Phys. **A158**, 309 (1970); A. M. Cormack, J. N. Palmieri, N. F. Ramsey, and Richard Wilson, Phys. Rev. **115**, 599 (1959); J. N. Palmieri, R. Goloskie, and A. M. Cormack, Phys. Lett. **6**, 289 (1963); O. N. Jarvis and B. Rose, *ibid.* **15**, 271 (1965).

[17]For example, J. J. Griffin, Phys. Rev. Lett. **17**, 478 (1966); Phys. Lett. **24B**, 5 (1967); Marshall Blann, Phys. Rev. Lett. **21**, 1357 (1968); **27**, 337 (1971); **28**, 757 (1972); M. Blann and A. Mignerey, Nucl. Phys. **A186**, 245 (1972).

[18]For example, Hugo W. Bertini, Phys. Rev. **131**, 1801 (1963).

[19]For example, P. G. Roos, N. S. Chant, D. W. Devins, D. L. Friesel, W. C. Jones, A. C. Attard, R. S. Henderson, I. D. Svalbe, B. M. Spicer, V. C. Officer, and G. G. Shute, Phys. Rev. Lett. **40**, 1439 (1978); J. W. Watson, M. Ahmed, D. W. Devins, B. S. Flanders, D. L. Friesel, N. S. Chant, P. G. Roos, and J. Wastell, Phys. Rev. C **26**, 961 (1982); C. Samanta, Ph.D. thesis, University of Maryland, 1981; L. Rees, Ph.D. thesis, University of Maryland, 1983.

[20]Th. A. J. Maris, Nucl. Phys. **9**, 577 (1958); Daphne F. Jackson and Tore Berggren, *ibid.* **62**, 353 (1965); N. S. Chant and P. G. Roos, Phys. Rev. C **15**, 57 (1977).

[21]G. F. Bertsch and O. Scholten, Phys. Rev. C **25**, 804 (1982).

[22]N. S. Chant and P. G. Roos, Phys. Rev. C **27**, 1060 (1983).

[23]N. S. Chant, P. Kitching, P. G. Roos, and L. Antonuk, Phys. Rev. Lett. **43**, 495 (1979).

[24]T. K. Lim, Nucl. Phys. **A129**, 259 (1969); Phys. Lett. **43B**, 349 (1973); **44B**, 341 (1973).

[25]B. S. Podmore and H. S. Sherif, *Few Body Problems in Nuclear and Particle Physics,* edited by R. J. Slobodrian, B. Cujec, and K. Ramavataram (Université Lavel, Quebec, 1975), p. 517.

[26]W. T. H. van Oers, B. T. Murdoch, B. K. S. Koene, D. K. Hasell, R. Abegg, D. J. Margaziotis, M. B. Epstein, G. A. Moss, L. G. Greeniaus, J. M. Breben, J. M. Cameron, J. G. Rogers, and A. W. Stetz, Phys. Rev. C **25**, 390 (1982).

[27]E. A. Rembler and R. A. Miller, Ann. Phys. (N.Y.) **82**, 189 (1974).

[28]R. Frascaria, P. G. Roos, M. Morlet, N. Marty, A. Willis, V. Comparat, and N. Fugiwara, Phys. Rev. C **12**, 243 (1975).